Table S1. DNA sequence of a synthetic *mGluR1* promoter.

Table S2. Transgene expression in selected retinal cell types after intraocular injection of adeno-associated virus into the eyes of adult mice

Figure S1. Including the nucleus minimally affects measurements of fluorescence change.

Figure S2. *mGluR6* promoter targets GCaMP3 expression to ON-type bipolar cells.

Figure S3. Distribution density and expression levels are highest around the virus injection site.

Figure S4. Tracing calcium signals from dendrites to soma.

Figure S5. Fluorescence increase in a dendrite precedes fluorescence increase in the soma.

Figure S6. Neural response modulation outside the temporal bandwidth of GCaMP3 increases fluorescence intensity.

Figure S7. Expression pattern of two viral vectors administered simultaneously.

Figure S8. Optical recording from retinal slice preparation minimizes scan laser artifacts.

Movie S1. Two-photon image series of the light flash-evoked GCaMP3 response recorded from photoreceptor terminals (rods and cones).

Movie S2. Two-photon image series of the light flash-evoked GCaMP3 response recorded from a horizontal cell soma and neurites.

Movie S3. Two-photon image series of the light flash-evoked GCaMP3 response recorded from an axonal arbor of an ON-type bipolar cell.

Movie S4. Two-photon image series of the light flash-evoked GCaMP3 response recorded from the soma and proximal lobules of a type-AII amacrine cell.

Movie S5. Two-photon image series of the light flash-evoked GCaMP3 response recorded from a small population of ganglion cells.

Movie S6. Two-photon image series of the light flash-evoked GCaMP3 response recorded from a larger population of ganglion cells.

Supplemental movies are available online at: http://www.bartborghuis.com/Supp/

tcactctagtgttttcatgtgacctcttgttctcaatttagatacttcttgacctggaaaaggtgggtgctgcttgccactctacatttggctactcctgtttt
aggatgtgcatgttccttcctcccccttgtctcccgccatgaaatctcttcccatcctctttgcaacctgacaacagagccttgtccctaggtagatatacac
atacattgtttttctcattgtgttccttatttttagagagagaaaaaaaatctgagtctgtaagataaatgcaaaggataacaatccccaaaacagcct
aggaacccctcattcctctggcaagacactactgatgatctgtatgcttggtagcctctttaagtcctctcagagatagtatagtagttgacaaatgc
cagctcctatattctctagcttctccttttcctctatcaaatgacttttaaataaattagatattagacaaaccttgggtgacctgctttttctttttctttttcctttt
ttttttttttacttctccccccgccccccctccccccccgttttttttcccttgcggtataatagtgttgaagaaagagggcactagtgtacagcccagatgg
cagccttgcaccgtctgatttggagctgaggtgtctgcgaaccgagggcggctgcagtcctctgacctgagaccaatagctctgtctacccggac
tcaggtaggtcttgaagatgaaagggtgtgtgtgtgtgtgtgtgtgtgtgtgtgtgtgtgtgtgtgtgtgtgtgtacgcgcgcgcgcgc
gcgagtgtacgaatcctagctctgagcgctgtccagggttctgacatttgagtggctcaggcggttcaagccccaacacagggaggctaccag
gcgttgccttagtaactaatatggcttttccacaagctgtcgcatttacattttccaccatcagcgtccagcttatggccactaacgcgccgctcattgca
cacctgattcacacaccttcgggcaccagtgaaaaaaccgcgacttgattttctggaagaacacccctagggtttgggagcggtcgtggaggga
ccagcaggaagaagcggaggggagaggggcggtggtggagactgagaagctttgaaccagctgtgttggccaaaggcacgaagcg
gcaaaagacagcggcgggcgtcagggtggttcgcgctgggaacctgcaggcgggaccggcgtgggaacgtggcttgccggcggtcga
accgcgtcttc

Table S1. DNA sequence of a synthetic *mGluR1* promoter. This promoter, packaged into an AAV2/1 vector, drove strong transgene expression in type AII amacrine cells.

Serotype	Ganglion cells	Amacrine cells	Bipolar cells	Horizontal cells	Rods & cones	Müller glia
AAV2/1	++	-	-	+	-	-
AAV2/2	+	-	-	-	-	-
AAV2/5	++	+	-	+	-	+
AAV2/7	-	-	-	-	-	-
AAV2/9	++	-	-	+	++	-

Table S2. Transgene expression in selected retinal cell types after intraocular injection of adeno-associated virus into the eyes of adult mice. In all vectors, transgene expression was driven by the mouse *synapsin-1* promoter. Expression was evaluated as the number of visibly labeled neurons 14 days after injection and reported as follows: none detected (-); 1 to 100 (+); 100 to 5000 (++).

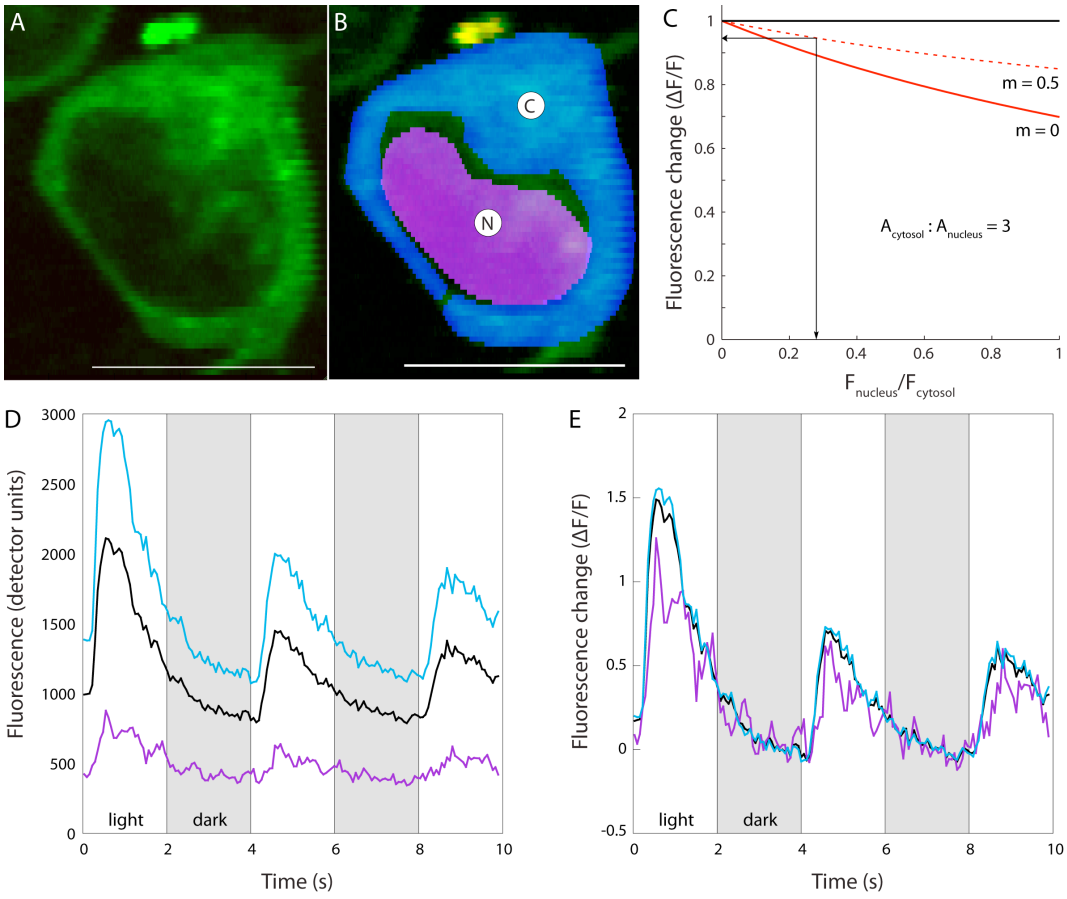

Figure S1. Including the nucleus minimally affects measurements of fluorescence change. The nucleus of a GCaMP3-expressing neuron is typically devoid of fluorescent sensor protein (>3-fold dimmer than the surrounding cytosol). For measuring fluorescence responses, this raises the question how much fluorescence measurements change when the nucleus is included in the analyzed region of interest (ROI). This question is pertinent because accounting for the nucleus requires an additional step in the annotation process, which might be a constraint for the analysis of large numbers of neurons. **A** Fluorescence image of a recorded ganglion cell. **B** ROIs covering the cytosol (C, blue) and nucleus (N, magenta) of the cell shown in A. **C** Model simulation of the expected effect of the nucleus on measured fluorescence change. ΔF/F of the cytosol was fixed at 1; the ratio of cytosol to nucleus pixel area was 3 (measured from the cell in panel A). Relative baseline fluorescence of the nucleus was varied from 0 (dark) to 1 (equal to cytosol). The black line represents ΔF/F of the cytosol alone; the red lines represent measurements that include the nucleus. In one case, fluorescence in the nucleus does not modulate (m = 0, solid), in the second case fluorescence in the nucleus modulates with a ΔF/F of 0.5 (m = 0.5 dotted). For values obtained from our data, this simple model shows that including the nucleus in the ROI will decrease measured ΔF/F by ~5%. **D** Fluorescence intensity measured from the cell shown in panel B (ON cell) in the presence of a light stimulus that switched from bright to dim and *vice versa* every two seconds. **E** Change in fluorescence calculated from the data shown in D. Values measured from cytosol alone, and cytosol + nucleus vary little. ΔF/F of the nucleus is similar to that of the cytosol, but it is noisier due to increased quantal noise associated with lower photon flux.

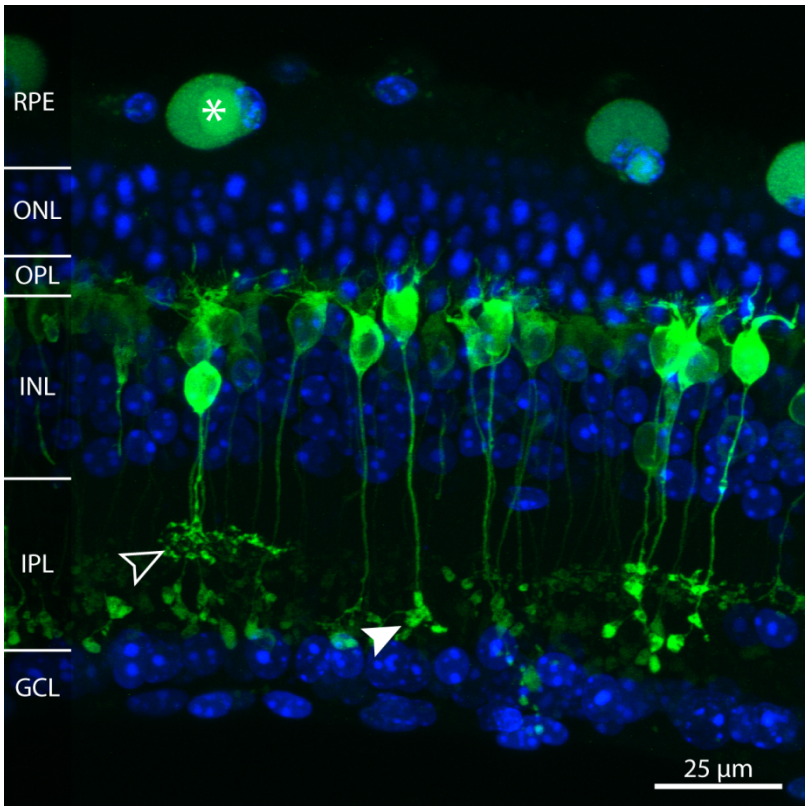

Figure S2. *mGluR6* promoter targets GCaMP3 expression to ON-type bipolar cells. Z-projection of confocal image stack of a retinal slice preparation six weeks after sub-retinal electroporation of vector plasmid p-*mGluR6*-GCaMP3 in a p0 mouse pup. Image shows the dendrites, somas and synaptic terminals of GCaMP3 (green) expressing bipolar cells and some autoflourescent retinal pigment epithelial cells (asterisk). Blue: nuclear stain (DAPI). The section contains many bipolar cells whose axonal arborizations are restricted to the ON sublamina. This includes rod bipolar cells, whose axon terminals (solid arrowhead) arborize in stratum 5 of the IPL, nearest to the ganglion cell layer and cone bipolar cells, whose axon terminals (open arrowhead) stratify in strata 3 and 4 of the IPL.

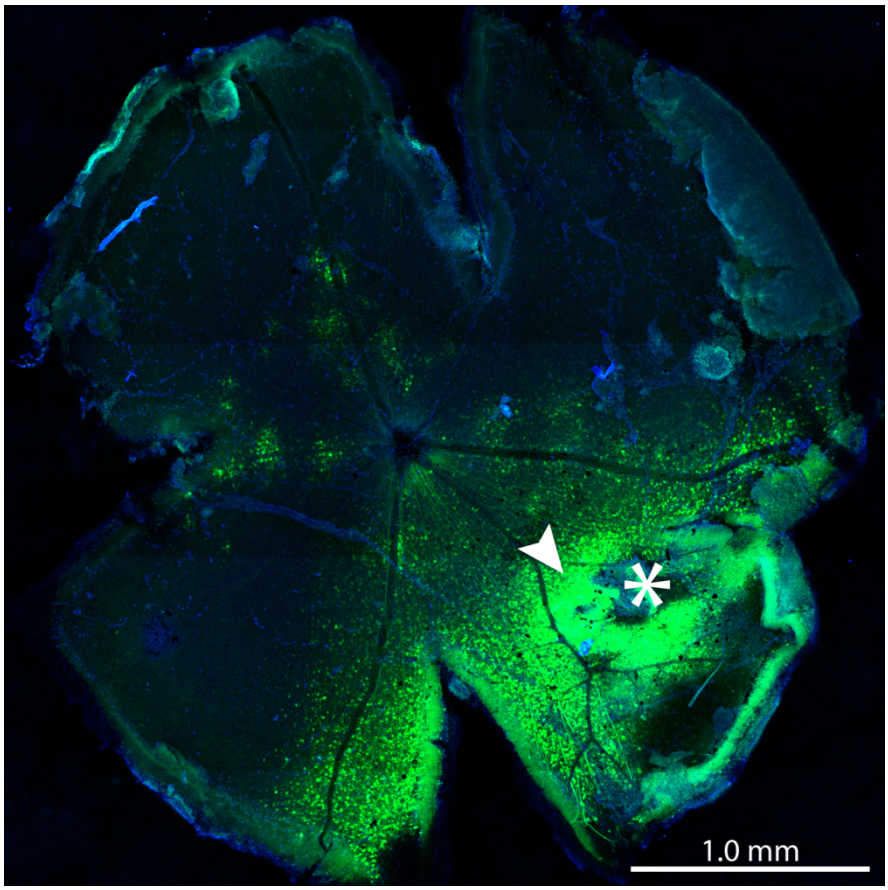

Figure S3. Distribution density and expression levels are highest around the virus injection site. Confocal image of a whole-mount retina with GCaMP3-expressing neurons (green) counter-stained with the nuclear stain DAPI (blue). To inject AAV2/1-*syn1*-GCaMP3 into the vitreous body of the eye of an anesthetized mouse, the sclera and retina near the *ora serrata* were punctured with a 30 gauge sharp needle. Then, a 33 gauge blunt tipped needle attached to an injection syringe was inserted into the vitreous body and a small volume of virus in suspension injected (0.8 µl). Retinas typically showed strong fluorescence labeling and a high distribution density of transduced cells (arrowhead) around the penetration site (asterisk).

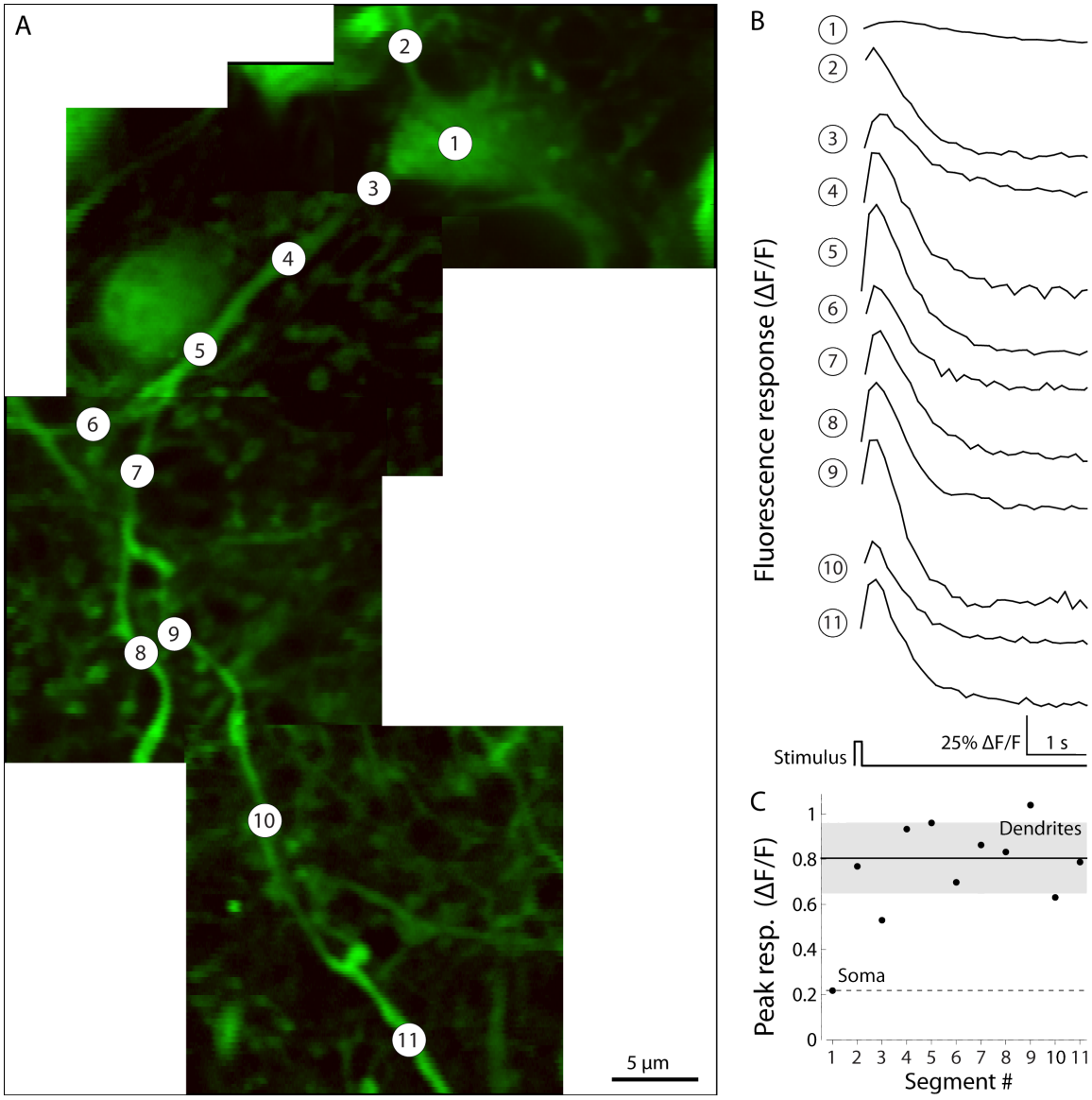

Figure S4. Tracing calcium signals from dendrites to soma. A. Two-photon fluorescence image reconstruction of a ganglion cell soma (1) and its primary dendrites (2-11). **B.** Fluorescence response to a brief light flash recorded in the dendritic segments indicated in A (each trace represents the average of > 6 trials). Dendritic fluorescence responses were consistently larger in amplitude and shorter in their rise- and decay times than the simultaneously imaged soma. **C.** Peak amplitude of the fluorescence responses shown in B. Solid black line, average Δ*F*/*F* of all dendritic segments; gray area, mean ± 1 s.d.

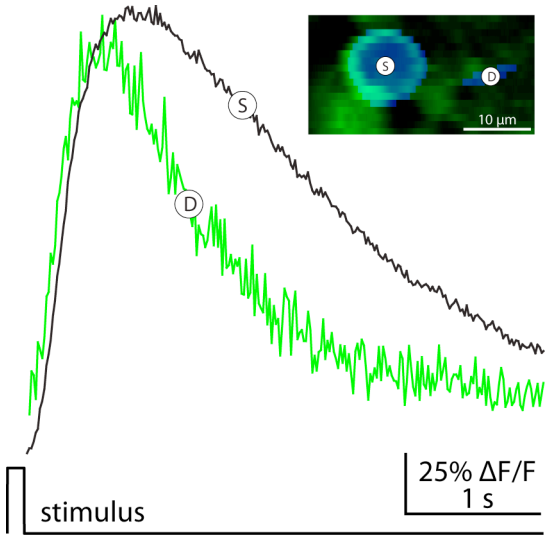

Figure S5. Fluorescence increase in a dendrite precedes fluorescence increase in the soma. Peak-normalized fluorescence response of soma (S) and dendrite (D; two-photon image shown in inset) recorded at 60 frames s^{-1}. The rising phase of the signal recorded in the dendrite (green) leads the rising flank recorded simultaneously in the soma (black) by 58 ms. The fluorescence response in the dendrite peaks 144 ms before the soma. Respective decay time constants of the signal recorded in dendrite and soma are 0.82 and 1.90 s.

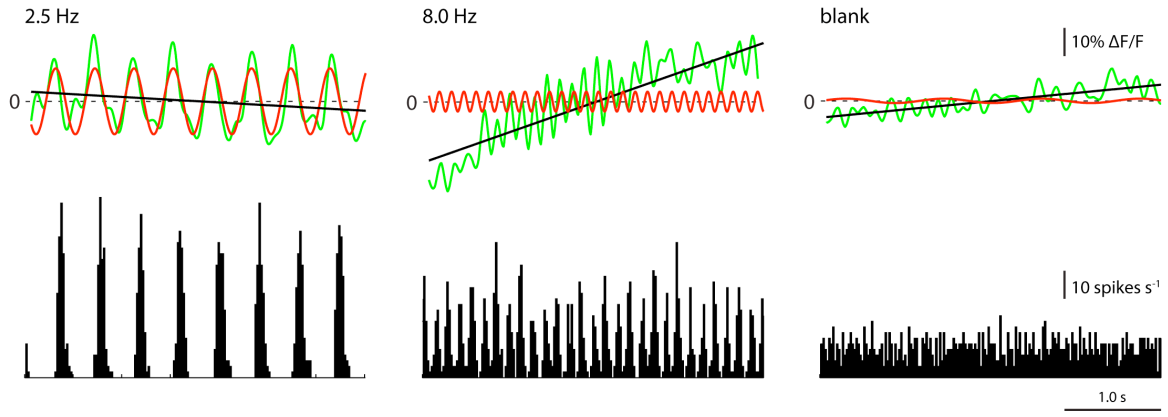

Figure S6. Neural response modulation outside the temporal bandwidth of GCaMP3 increases fluorescence intensity. Comparison of the spike response (bottom; black, PSTH) and fluorescence signal (top; green) in a ganglion cell stimulated with a drifting sinusoidal grating temporally modulated at 2.5 or 8 Hz. Right panel shows the cell's baseline response in the presence of a gray screen (same mean luminance as grating stimuli). While PSTHs show strong response modulation at both temporal frequencies (left and middle panels), the modulation amplitude of the fluorescence signal is greater by >3 fold for the low compared with the high frequency stimulus (red, Fourier amplitude of fluorescence response at dominant frequency). Average fluorescence does not change appreciably for the low frequency stimulus, whereas the high frequency stimulus evokes an increase in the average fluorescence. This increase is consistent with integration of the stimulus-evoked calcium response over time. The increase is less apparent in the spontaneous signal (right panel), where the spike rate is low and unmodulated. The slight fluorescence increase during spontaneous firing can be ascribed to increased spiking evoked by the scan laser.

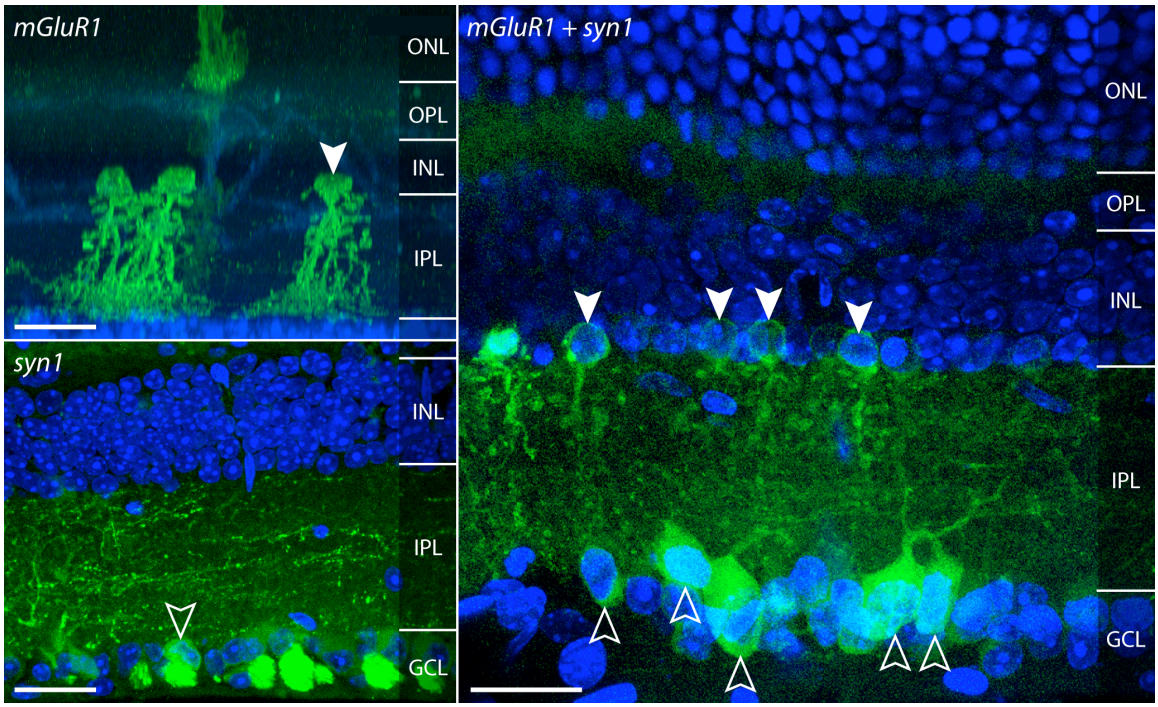

Figure S7. Expression pattern of two viral vectors administered simultaneously. Confocal images of retinas transduced with: top left, AAV2/1-*mGluR1*-GCaMP3, which is expressed in type AII amacrine cells (solid arrowhead); bottom left, AAV2/1-*syn1*-GCaMP3, which is expressed in ganglion cells (open arrowhead); and right, AAV2/1-*mGluR1*-GCaMP3 + AAV2/1-*syn1*-GCaMP3. Combining the two vectors results in a retina where both type AII amacrine cells and ganglion cells are labeled (respectively solid and open arrowheads). Retinas were counterstained with DAPI (blue). All images are projections of 10 µm thick confocal stacks (10 µm). Scale bars = 25 µm.

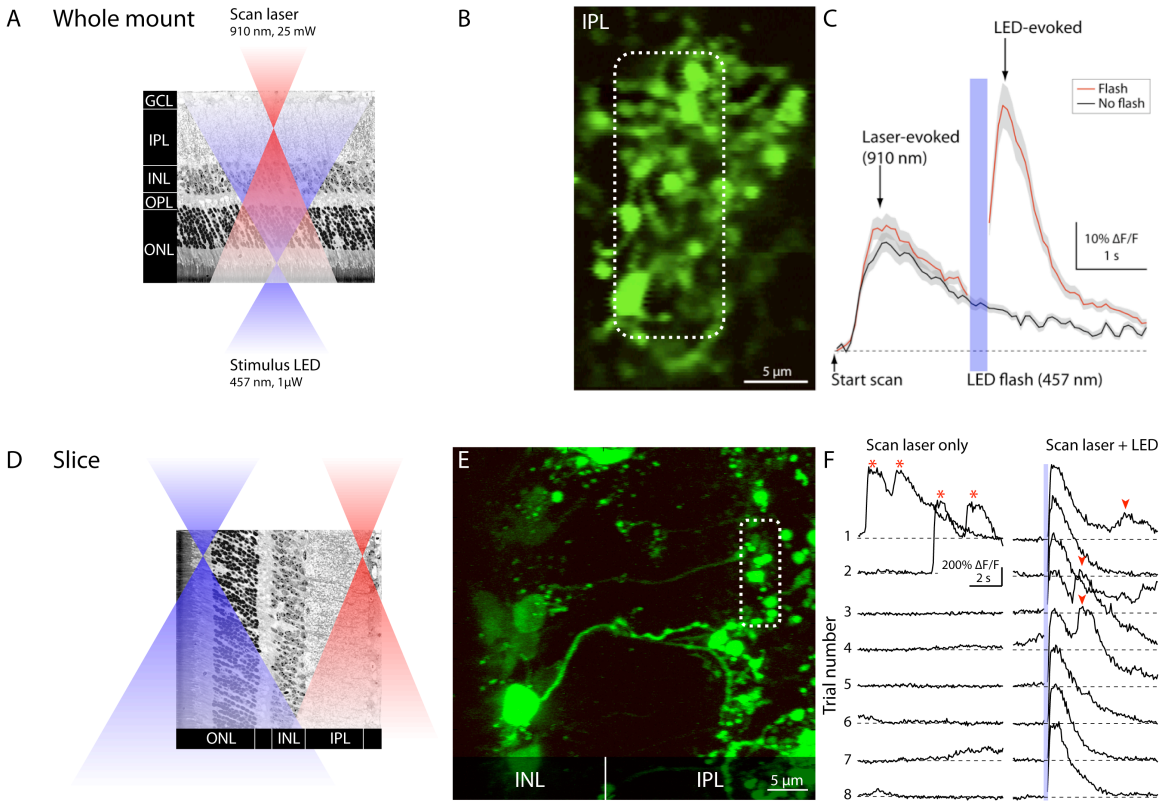

Figure S8. Optical recording from retinal slice preparation minimizes scan laser artifacts. Comparison of optical responses recorded from the axonal arbors (synaptic terminals) of GCaMP3-expressing ON-type bipolar cells. **A-C**. In a whole mount preparation, the scan area is concentric with the photoreceptors driving neurons in the optically recorded area. Because the scan laser activates the photoreceptors, a response synchronized to laser onset is observed at the start of each recording (C). **D.** This laser-evoked response is absent in recordings from a retinal slice, where the photoreceptors driving the recorded neurons lie outside the region exposed to the scan laser. **E.** Two-photon fluorescence image of a recorded bipolar cell. Dotted rectangles show ROIs used to measure the fluorescence response shown in E. **E.** Fluorescence response in the presence and absence of LED stimulation (traces show single trials). The first two trials in the laser-only configuration show response events (asterisks) that are not synchronized to scan laser onset and are interpreted as spontaneous release. These quantal-like response events were observed only in this cell type and therefore may reflect a feature that is specific to the rod bipolar synapse. It is consistent with 'all or none' signaling due to the rod's high-gain input synapse. The LED stimulus evoked a robust response (typical $\Delta F/F >> 100$). On some trials, the light-evoked response was followed by a second peak (arrowhead) similar to those in the scan laser-only condition.